

1 **Climate reconstruction from paired oxygen-isotope analyses of chironomid larval head**  
2 **capsules and endogenic carbonate (Hawes Water, UK) - potential and problems**

3

4 Alex Lombino<sup>1</sup>, Tim Atkinson<sup>1,2</sup>, Stephen J. Brooks<sup>3</sup>, Darren R. Gröcke<sup>4</sup>, Jonathan Holmes<sup>1</sup>,  
5 Vivienne J. Jones<sup>1</sup>, Jim D. Marshall<sup>5</sup>, Klaas G.J. Nierop<sup>6</sup>, Zoë Thomas<sup>7</sup>

6

7 <sup>1</sup>Environmental Change Research Centre, Department of Geography, University College  
8 London, Gower Street, London, WC1E 6BT, UK

9 <sup>2</sup>Department of Earth Sciences, University College London, Gower Street, London, WC1E  
10 6BT, UK

11 <sup>3</sup>Department of Life Sciences, Natural History Museum, Cromwell Road, London SW7 5BD,  
12 UK

13 <sup>4</sup>Department of Earth Sciences, Durham University, South Road, Durham, DH1 3LE, UK

14 <sup>5</sup>Department of Earth, Ocean and Ecological Sciences, University of Liverpool, Liverpool, L69  
15 3GP, UK

16 <sup>6</sup>Department of Earth Sciences and GeoLab, Faculty of Geoscience, Utrecht University,  
17 Princetonlaan 8, 3584 CB Utrecht, the Netherlands

18 <sup>7</sup>School of Biological, Earth and Environmental Science, University of New South Wales,  
19 NSW Australia 2052

20

21

22

23

24

25

26 **ABSTRACT**

27 Temperature and the oxygen isotopic composition ( $\delta^{18}\text{O}$ ) of meteoric water are both important  
28 palaeoclimatic variables, but separating their influences on proxies such as the  $\delta^{18}\text{O}$  of lake  
29 carbonates is often problematic. The large temperature variations that are known to have  
30 occurred in the northern mid-latitudes during the Late Glacial make this interval an excellent  
31 test for a novel approach that combines oxygen-isotope analyses of chironomid larval head  
32 capsules with co-occurring endogenic carbonate. We apply this approach to a Late Glacial lake  
33 sediment sequence from Hawes Water (NW England). Oxygen-isotope values in chironomid  
34 head capsules show marked variations during the Late Glacial that are similar to the oxygen  
35 isotope record from endogenic carbonate. However, summer temperature reconstructions  
36 based on the paired isotope values and fractionation between chironomids and calcite yield  
37 values between  $-20$  and  $-4^\circ\text{C}$ , which are unrealistic and far lower than reconstructions based  
38 on chironomid assemblages at the same site. The composition of a limited number of samples  
39 of fossil chironomid larval head capsules determined using Pyrolysis gas-chromatography  
40 mass spectrometry indicates the presence of aliphatic geopolymers, suggesting that diagenetic  
41 alteration of the head capsules has systematically biased the isotope-derived temperature  
42 estimates. However, a similar trend in the isotope records of the two sources suggest that a  
43 palaeoclimate signal is still preserved.

44

45 Keywords: oxygen isotopes; chironomids; Late Glacial; NW England; lake sediments;  
46 palaeotemperature

47

48

49

50

51

## 52 **1. Introduction**

53 Variations in oxygen isotopic composition of lake sediments provide an excellent means of  
54 past climate reconstruction. Analyses are most commonly undertaken on endogenic or biogenic  
55 carbonate (Leng and Marshall, 2004), although other lacustrine materials have also been used,  
56 including biogenic silica (Leng and Barker, 2006), aquatic cellulose (Wolfe et al., 2007; Heyng  
57 et al., 2014) and chitin (Wooller et al., 2004). Oxygen isotopes have an advantage over many  
58 other climate proxies in that their distribution is governed by well-understood physical  
59 principles and in favourable cases they can be used to make quantitative reconstructions with  
60 well-defined uncertainties. For lacustrine carbonates however, the interpretation of oxygen-  
61 isotope records is confounded by the fact that  $\delta^{18}\text{O}_{\text{carbonate}}$  is controlled both by water  
62 temperature and water isotope composition, as well as possible departures from isotopic  
63 equilibrium (Leng and Marshall, 2004). Deconvolving the signature into its individual  
64 components is difficult without independent estimates of either past water temperature or  
65  $\delta^{18}\text{O}_{\text{lakewater}}$ , which may not be available. Moreover, although carbonate-precipitating lakes are  
66 not uncommon, most lakes in acidic catchments do not precipitate carbonates and in these cases  
67 other materials must therefore be used to construct oxygen-isotope records.

68

69 The chitinous remains of chironomid larvae (Insecta: Diptera: Chironomidae) provide an  
70 alternative and promising means for inferring past  $\delta^{18}\text{O}_{\text{lakewater}}$ . The fractionation of oxygen-  
71 isotopes between chitin and water has been thought to be negligibly affected by temperature  
72 (Mayr et al., 2015). If this assumption were true,  $\delta^{18}\text{O}_{\text{chironomid}}$  values could be used to estimate  
73  $\delta^{18}\text{O}_{\text{lakewater}}$  without the need for an independent estimate of water temperature. Lombino et al.  
74 (2021) have recently provided evidence for a small temperature dependence of oxygen-isotope  
75 fractionation between chironomid head capsules and water. In either circumstance, there exists

76 the potential to combine  $\delta^{18}\text{O}_{\text{chironomid}}$  and  $\delta^{18}\text{O}_{\text{carbonate}}$  values from the same levels in a  
77 stratigraphic sequence in order to reconstruct past water temperature. Although paired  
78  $\delta^{18}\text{O}_{\text{chironomid}}$  and  $\delta^{18}\text{O}_{\text{carbonate}}$  analyses have previously been reported from a Quaternary  
79 sediment sequence (Verbruggen et al., 2010), no attempt has yet been made to undertake  
80 quantitative temperature reconstructions using such an approach, nor to evaluate its validity.  
81 In this study, we undertook such paired analyses from the Late Glacial sediments of Hawes  
82 Water, a small hardwater lake in NW England, in order to reconstruct the  $\delta^{18}\text{O}_{\text{lakewater}}$  and lake  
83 water temperature. For evaluation of this new approach, Hawes Water has the advantage of  
84 previously-published and methodologically-independent estimates of palaeotemperature,  
85 undertaken using transfer-functions based on the species compositions of chironomid  
86 assemblages (Marshall et al., 2002; Jones et al., 2002; Bedford et al., 2004; Lang et al., 2010),  
87 against which the results of our isotope-based calculations can be compared.

88

89 The Late Glacial, which is taken here to refer to the interval between the onset of warming at  
90 the end of Greenland Stadial 2 (GS-2) and the start of the Holocene (~14.7 – 11.7 ka BP), was  
91 a time of rapid, high-amplitude change in temperature in the boreal mid- and high latitudes  
92 (Lowe et al., 2008) and thus represents an excellent testing ground for our approach.  
93 Temperature reconstructions from chironomid assemblages indicate that during the Late  
94 Glacial interstadial mean July air temperatures in northwest England were between ~11 and  
95 14°C, falling to between ~7 and 10°C during the Younger Dryas stadial and then rising again  
96 to between ~11.5 and 15°C in the Early Holocene (Brooks and Langdon, 2014). These  
97 substantial temperature changes should be mirrored in the oxygen-isotope ratios of both  
98 endogenic carbonates and chironomid chitin. To be judged successful, any isotope-based  
99 method of temperature reconstruction should be capable of accurately matching the transfer  
100 function results for summer air temperatures. There is additional evidence that the Late Glacial

101 climate was characterized by changes in atmospheric circulation (e.g. Bakke et al., 2009; Lane  
102 et al., 2013). As oxygen isotopes in meteoric waters are sensitive tracers of atmospheric  
103 circulation (e.g. Hammarlund et al., 2002), concomitant reconstruction of lake water  $\delta^{18}\text{O}$  from  
104 paired chironomid and carbonate values might provide new information for comparison with  
105 previous studies.

106

## 107 **2. Study site, materials and methods**

### 108 2.1 Hawes Water and the Late Glacial sediment record

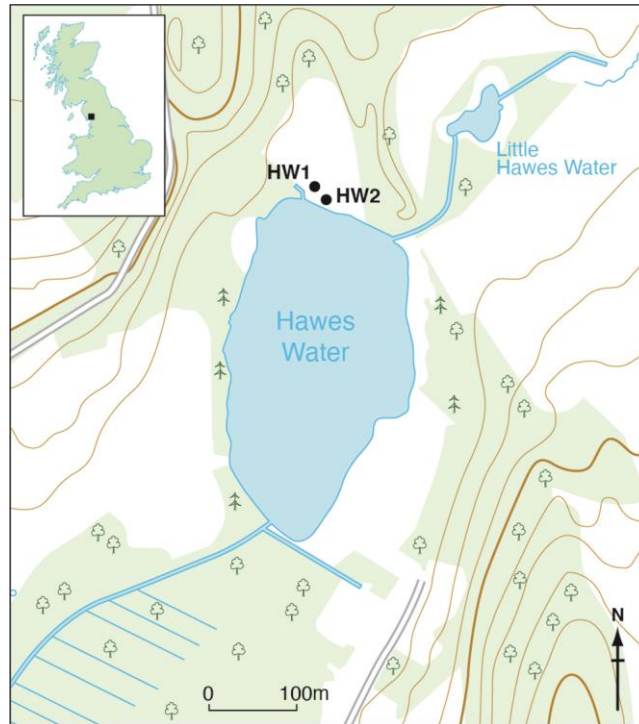
109 Hawes Water (54°10'58"N, 2 48'10"W) is a small, oligotrophic, monomictic lake (area 0.08  
110 km<sup>2</sup>, max depth ~12 m, 8 m a.s.l.) situated within a Carboniferous limestone catchment in  
111 north-west England (Marshall et al., 2002; 2007) (Fig. 1). The surface catchment area is small  
112 and boggy and the principal inputs to the lake are groundwater flow from the Carboniferous  
113 limestone as well as rainwater falling onto the lake and its catchment. The lake has a residence  
114 time of <1 year (Wiik et al., 2015). Although NW England was ice-covered during the last  
115 glacial, the Hawes Water catchment was free of ice by the Late Glacial (Jones et al. 2002). The  
116 weighted mean annual  $\delta^{18}\text{O}$  of precipitation (2003–2005) is -6.8 ‰ VSMOW, with slightly  
117 higher (-6.1 ‰) values during summer over the same period. Summer epilimnion waters (-5.3  
118 ‰, 1998–2005) show slight evaporative enrichment with respect to rainfall and modern calcite  
119 precipitates in oxygen-isotope equilibrium with those waters (Marshall et al., 2007). Marshall  
120 et al. (2007) also present results of several years of monitoring of the lake and its environment  
121 and note that in summer the temperature difference between lake waters and the air above  
122 averages 2.3°C.

123

124 This study is based on data derived from three cores (HW1/1 and HW1/2, which are referred  
125 to collectively as HW1 below, and HW2), all taken within a few meters of each other from the

126 marl benches slightly landward of the northern margins of the present lake (Fig. 1). These  
127 benches formed under shallow water when lake-levels were higher during the Late Glacial.  
128 Between about 1.0 and 1.3 m of characteristic tri-partite Late Glacial and early Holocene  
129 sediment (marl-clay-marl) is present in each sequence, overlying blue clays deposited at the  
130 end of the last glacial. Marl sediments are overlain by fen peat, which formed when lake levels  
131 fell during the very early Holocene (Jones et al., 2011). The Late Glacial carbonate sediments  
132 formed endogenically within the lake, with no evidence for input of detrital carbonate from the  
133 catchment (Marshall et al., 2002). As part of this study, Core HW2 (107 cm long) was  
134 recovered for chironomid oxygen-isotope analyses using a large-diameter ‘Russian’ corer:  
135 carbonate oxygen-isotope analyses were also undertaken on this material. Complementary  
136 published data are available from parallel, ~120 cm long cores HW1/1 and HW1/2: carbonate  
137 oxygen-isotopes were undertaken on the former (Jones et al., 2002; Marshall et al., 2002) and  
138 chironomid-inferred temperatures determined on the latter (Bedford et al., 2004). The two  
139 datasets were placed on a common depth scale to allow for minor differences in depth, as  
140 described in Bedford et al. (2004). Cross correlation of the HW1 sequence with HW2 was  
141 achieved by sequence-slotting (see Supplementary Material) of the carbonate oxygen-isotope  
142 data from the two cores.

143



144

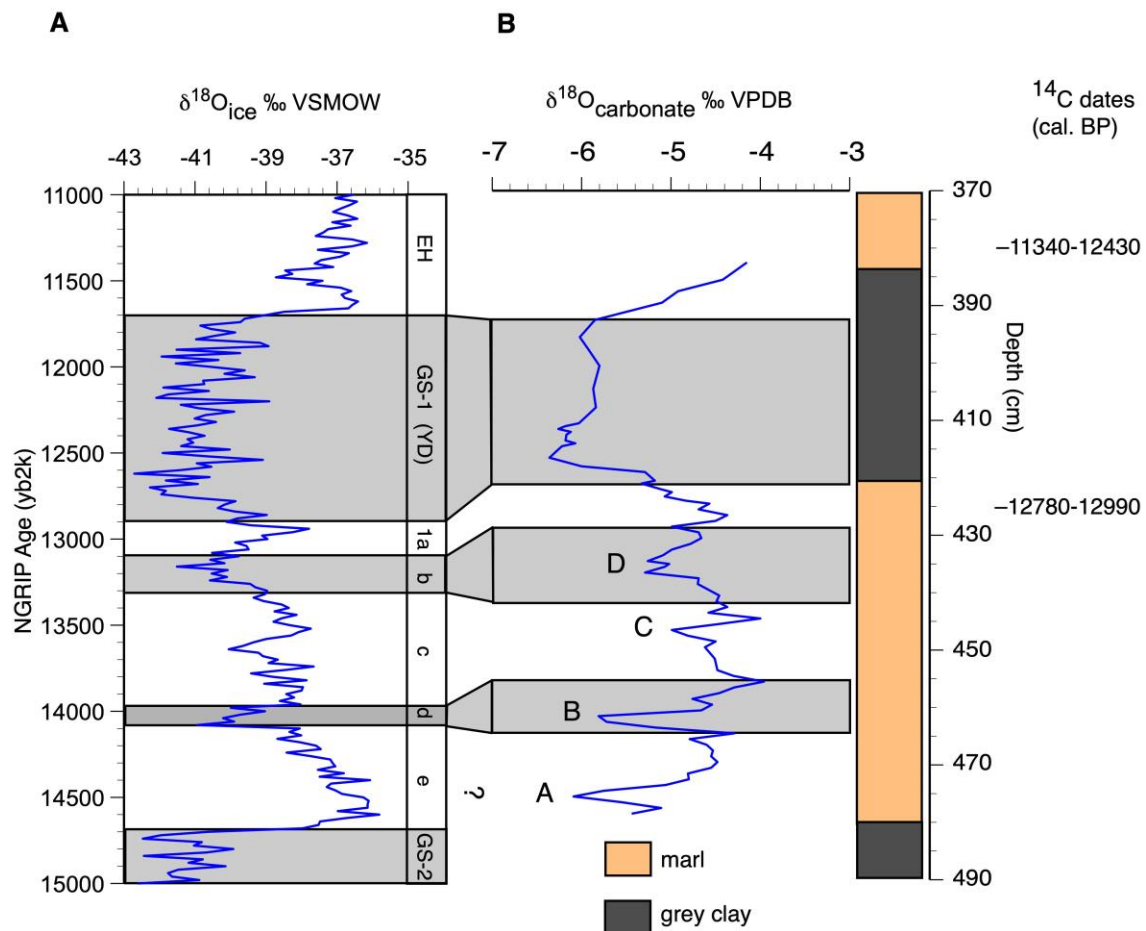
145 Fig. 1. Location of the coring sites at Hawes Water. Inset shows the location of the lake in NW  
 146 England.

147

## 148 2.2 Chronology and Late Glacial environment at Hawes Water

149 Previously-published lithological information, pollen,  $\delta^{18}\text{O}_{\text{carbonate}}$  and chironomid-inferred  
 150 temperatures on HW1/1 and HW1/2 were compared by Lang et al. (2010) with the oxygen-  
 151 isotope event stratigraphy for the NGRIP ice core (Lowe et al., 2008) in order to develop a  
 152 chronology for the Late Glacial sequence at Hawes Water, with confirmation of a late glacial  
 153 age provided by two radiocarbon dates on terrestrial plant macrofossils (Marshall et al., 2002)  
 154 (Fig. 2). The studied sequence begins with marl corresponding to the Late Glacial interstadial,  
 155 overlying clays deposited during Greenland Stadial 1. There is an initial rise in  $\delta^{18}\text{O}_{\text{carbonate}}$  in  
 156 the marl that was abruptly followed by a temporary reversal (marked “A” on Fig. 2) before the  
 157  $\delta^{18}\text{O}_{\text{carbonate}}$  rise was resumed. Over the same interval, there was an increase in head capsules  
 158 from thermophilic chironomid taxa (Bedford et al., 2004). The published pollen record  
 159 indicates open grassland during this interval (Jones et al. 2002; Bedford et al., 2004), which

160 marks the transition from the glacial into the Late Glacial interstadial (Greenland Interstadial  
161 1a to 1e). Marl continues above this, with high  $\delta^{18}\text{O}_{\text{carbonate}}$  values that are interrupted by 3  
162 marked negative excursions (labelled “B”, “C” and “D” on Fig. 2). There is a large but  
163 progressively decreasing number of thermophilic chironomid taxa and pollen indicative of  
164 juniper scrub in the earlier part and birch woodland in the later part of the interval, which  
165 coincides with the Late Glacial interstadial. The uppermost part of the marl shows a sharp  
166 lowering of  $\delta^{18}\text{O}_{\text{carbonate}}$  values and a return to pollen indicative of open grassland vegetation  
167 coupled with a shift to fewer thermophilic and more cold-tolerant chironomid taxa. The  
168 overlying clay, which displays low  $\delta^{18}\text{O}_{\text{carbonate}}$  values, an abundance of cold-tolerant  
169 chironomid taxa and pollen indicative of open ground to tundra vegetation, coincides with the  
170 Younger Dryas stadial (Greenland Stadial 1). An increase in  $\delta^{18}\text{O}_{\text{carbonate}}$  values in the upper  
171 part of the clay, a shift to pollen indicative of open ground and an increase in warm-water  
172 chironomid taxa marks the transition to the Early Holocene, which is accompanied by a return  
173 to marl sedimentation, a rise in  $\delta^{18}\text{O}_{\text{carbonate}}$  values and a change to grassland pollen. Above  
174 this, marl sediments are replaced by Early Holocene fen peat.



175

176

177 Fig. 2. Development of a chronology for the Hawes Water Late Glacial sediment sequence. **A.**

178 Greenland ice core (NGRIP) oxygen-isotope record (North Greenland Ice Core Project

179 members, 2004), with proposed correlation to HW1. Shading denotes NGRIP stadials. GS2 =

180 Greenland Stadial 2; 1a to 1e inclusive = Greenland Interstadial 1a to 1e, which is equivalent

181 to the Late Glacial Interstadial; GS-1 (YD) = Greenland Stadial 1, which is equivalent to the

182 Younger Dryas Stadial; EH = Early Holocene. **B.** Late Glacial carbonate oxygen-isotope

183 record from Hawes Water core HW1 (on its original depth scale). Events labelled “A” to “D”

184 are negative oxygen-isotope excursions in the HW1 record (based on Marshall et al., 2002;

185 Lang et al., 2010). Radiocarbon dates are from Marshall et al. (2002), calibrated here using

186 Calib 8.20 (Stuiver and Reimer, 1993) and IntCal20 and expressed as 1 sigma ranges in

187 calendar years BP.

188

## 189 2.4 Analytical methods

190 The principal laboratory methods employed in this study were  $\delta^{18}\text{O}$  analysis of chironomid  
191 head capsules by pyrolysis to CO over carbon at 1450°C followed by gas-source mass  
192 spectrometry, and isotopic analysis of endogenic lake carbonate samples by conventional  
193 techniques. In addition, a few samples of chitin from head capsules were analysed by flash  
194 pyrolysis followed by gas chromatography and mass spectrometry (Py-GC-MS). The original  
195 purpose of the Py-GC-MS analyses was to compare the effects of different pre-treatments of  
196 the head capsules on the molecular degradation of chitin, but this method later provided  
197 important evidence for alteration of the original chitin in the Hawes Water samples.

198

### 199 2.4.1 Isotope analysis of chironomid head capsules

200 Freeze-dried, 1 cm-thick sediment segments from selected intervals were washed through 210  
201  $\mu\text{m}$  and 90  $\mu\text{m}$  mesh sieves with deionized water and sonicated to remove sediment particles.  
202 The stratigraphic resolution of the chironomid record was restricted by the abundance of  
203 chironomids; however, where possible, analyses were performed every 2 cm. Chironomid head  
204 capsules were picked from aliquots of sieved residue under a low-power ( $\times 25$  magnification)  
205 binocular microscope. Owing to limited availability of material, all the head capsules in each  
206 level were aggregated, regardless of species, and because of this species identifications were  
207 not determined. Based on experiments to determine minimum sample size and optimum  
208 methods for head capsule purification (Supplementary Material),  $60 \pm 10 \mu\text{g}$  of head capsule  
209 material from each sample was analyzed following pretreatment to eliminate impurities. The  
210 pretreatment process involved three steps applied sequentially to each sample of separated head  
211 capsules; firstly 2:1 dichloromethane:methanol, secondly 0.25 M HCl and thirdly 0.25 M  
212 NaOH for 24 hours at 20°C. The head capsules were further washed and sonicated at each stage

213 in the treatment process to confirm that all particles of sediment had been removed. Oxygen-  
214 isotope analyses of treated chironomid remains were performed at Durham University Stable  
215 Isotope Biogeochemistry Laboratory (SIBL) using a Thermo TC/EA coupled to a Thermo-  
216 Finnigan Delta V Advantage IRMS, via a ConFlo III interface. Oxygen-isotope ratios are  
217 expressed in standard delta units, as per mil (‰) deviations from the VSMOW standard.  
218 Results were calibrated against three international reference standards (IAEA-600, IAEA-601,  
219 IAEA-602). Sample analytical precision was better than  $< \pm 0.64$  ‰ (1 SD) based on analysis  
220 of three replicate samples from one level in the Hawes Water sequence that contained abundant  
221 chironomid head capsules.

222

#### 223 2.4.2 Isotope analysis of carbonate

224 Between 3 and 5 g aliquots of bulk sediment were treated with 100 mL 5% sodium hypochlorite  
225 overnight to remove organic material, wet-sieved through an 80  $\mu\text{m}$  mesh to remove bioclastic  
226 material, rinsed in deionized water and then freeze dried in order to isolate endogenic carbonate  
227 for oxygen-isotope analyses. Standard analytical methods were employed as described for the  
228 Hawes Water material in Marshall et al. (2002) and Thomas (2014). In brief, samples of around  
229 2 mg were then analyzed at the University of Liverpool stable isotope laboratory using a VG  
230 ISOCARB automated ‘common acid bath’ gas preparation system connected to a VG SIRA10  
231 mass spectrometer. Oxygen-isotope ratios are expressed in standard delta units, as per mil (‰)  
232 deviations from the VPDB standard. VPDB to VSMOW conversion, where required, followed  
233 Kim et al. (2015). Analytical precision for carbonates based on the long-term measurement of  
234 standards was better than  $\pm 0.1$  ‰ (1 SD).

235

236

237

238 2.4.3 Pyrolysis – gas chromatography – mass spectrometry (Py–GC–MS)

239 To monitor the effect of the combined purifications (extraction, acid and base treatment, see  
240 Supplementary Material) on their composition, modern chironomid head capsules and isolated  
241 fossil heads from three levels in the sequence (358 cm, 360 cm and 364 cm) were analysed by  
242 Py-GC-MS. The selection of core levels from which to analyse fossil heads was dictated by  
243 the availability of remaining material following the completion of the oxygen-isotope analyses.

244

245 Pyrolysis was carried out in helium carrier gas on a Horizon Instruments Curie-Point pyrolyser.  
246 Samples (typically 1–2 mg) were pressed onto Ni/Fe Curie point wires and subsequently heated  
247 for 5 s at 590°C. The pyrolysis unit was directly connected to a Carlo Erba GC8060 gas  
248 chromatograph through a splitless injector set at 280°C, and the products were separated by a  
249 fused silica column (Varian, 25 m, 0.32 mm i.d.) coated with CP-Sil5 (film thickness 0.40 µm).  
250 The GC oven was initially kept at 40°C for 1 min then heated at a rate of 7°C min<sup>-1</sup> to 320°C  
251 and maintained at that temperature for 15 min. The column was coupled to a Fisons MD800  
252 mass spectrometer (mass range *m/z* 45-650, ionization energy 70 eV, cycle time 0.7 s).  
253 Identification of the compounds was carried out from their mass spectra using a NIST library  
254 and/or by interpretation of the spectra, by their retention times and/or by comparison with data  
255 from the literature (Stankiewicz et al., 1996; Smith et al., 1988). Quantification was performed  
256 by peak integration using two main fragment ions of each compound. From the peak areas,  
257 relative contributions of each compound and groups of compounds were calculated using the  
258 correction factors reported by Menzel et al. (2005). Each day, prior to analysis of samples, a  
259 standard (ball-milled oak root, *Quercus robur* L.) was run in order to check pyrolysis,  
260 chromatography and mass spectrometry based on an array of compounds present, including  
261 polysaccharides, proteins, guaiacyl-lignin, syringyl-lignin, tannins, suberin, and triterpenoids.  
262 Each of these compounds has distinct features upon Py-GC-MS, thus allowing possible

263 problems with the system to be traced. In case of maintenance or when too much sample was  
264 pyrolyzed (based, for example, on peak overload or high intensity), a blank was run (either  
265 only GC-MS running or running a pre-extracted Curie-point wire). For the chitin-derived  
266 pyrolysis products correction factors were determined by dividing the peak area of the whole  
267 peak by those obtained from the selected fragment ions using the pyrolysis-GC trace of chitin  
268 powder. The correction factors are: acetic acid (1.5), acetamide (1.0), 3-acetamido-3-  
269 methylfuran (2.2), 3-acetamido-4-pyrone (3.1), and 1,6-anhydro-2-acetamido-2-deoxyglucose  
270 (5.4).

271

### 272 **3. Results and interpretation**

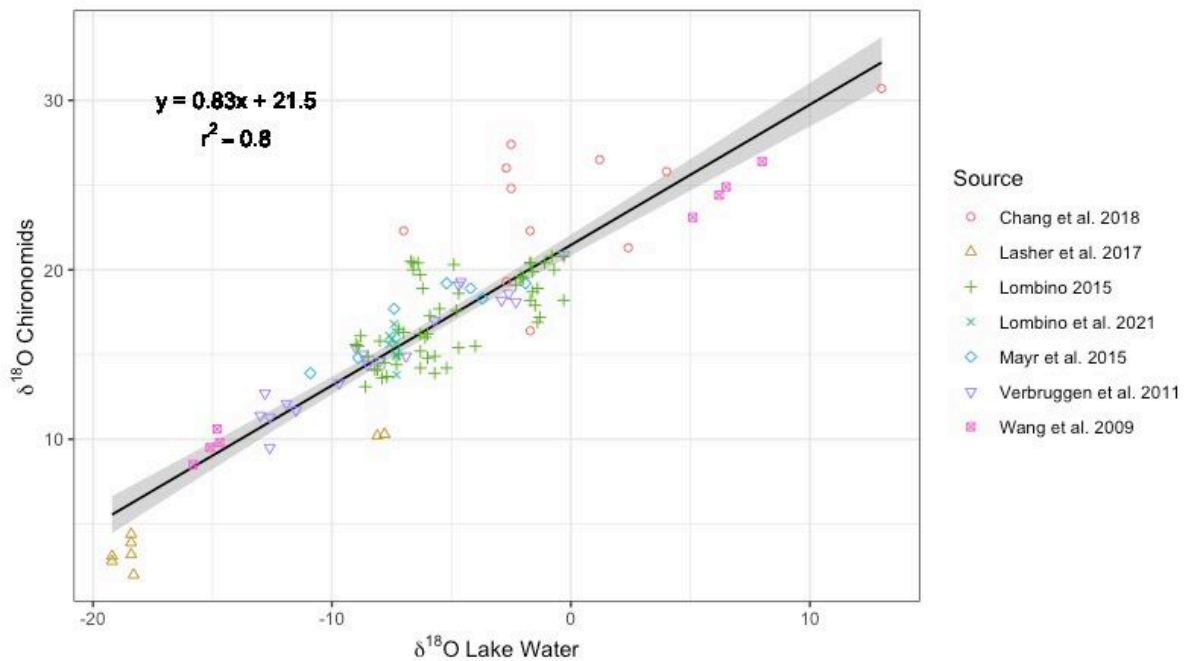
#### 273 3.1 Derivation of past water-temperature and lake water $\delta^{18}\text{O}$

274 Previous work has demonstrated a strong positive correlation between  $\delta^{18}\text{O}_{\text{chironomid}}$  and  
275  $\delta^{18}\text{O}_{\text{lakewater}}$  (van Hardenbroek et al., 2018). Fig. 3 combines information from the field  
276 collections reviewed by van Hardenbroek et al. (2018, see their Fig. 5) with data from  
277 laboratory culture experiments by Wang et al. (2009) and Lombino et al. (2021). Wang et al.  
278 (2009) performed experiments at constant temperature (25°C). Lombino et al. (2021) reared  
279 chironomid larvae in a range of cultures with temperatures from 5 to 25°C and found a small  
280 temperature effect of about  $-0.1 \text{‰ } ^\circ\text{C}^{-1}$ .

281

282 Although Fig. 3 reveals a strong relationship between  $\delta^{18}\text{O}_{\text{chironomid}}$  and  $\delta^{18}\text{O}_{\text{H}_2\text{O}}$ , the data also  
283 show considerable scatter ( $r^2 = 0.80$ ). This scatter probably results from a number of factors  
284 that differ both within and between the individual studies, including inter-species effects as  
285 well as differences in temperature, sample preparation methods and analytical protocols. The  
286 best-fit line does not indicate a 1:1 correspondence between the isotope ratios in the chironomid  
287 head capsules and the water, but instead has a gradient of 0.83. This probably reflects the fact

288 that in controlled culture experiments reported by Wang et al. (2009) about 30% of oxygen  
289 atoms in chironomid chitin were derived from their food, while 70% were derived from the  
290 host water. Differences in the isotopic composition of food consumed by the larvae in the  
291 various studies may also, therefore, have contributed to the scatter in Fig. 3.  
292



293  
294  
295 Fig. 3.  $\delta^{18}\text{O}_{\text{chironomid}}$  versus  $\delta^{18}\text{O}_{\text{H}_2\text{O}}$  based on a range of field collections (Verbruggen et al.,  
296 2011; Lombino, 2015; Mayr et al., 2015; Lasher et al, 2017; Chang et al., 2018) and two culture  
297 experiments (Wang et al., 2009 and Lombino et al., 2021). The ordinary least-squares  
298 regression line, with 95% confidence limits, was fitted through all of the data. Based on van  
299 Hardenbroek et al. (2018) with additions and modifications.

300  
301 The calcite–water ( $\alpha_{\text{calcite-H}_2\text{O}}$ ) and chironomid–water ( $\alpha_{\text{chironomid-H}_2\text{O}}$ ) oxygen-isotope  
302 fractionations can be combined in order to derive an estimate of water temperature, assuming  
303 that the calcite and the chironomids formed under the same temperature and water  $\delta^{18}\text{O}_{\text{H}_2\text{O}}$ .

304 Chironomid larvae generally live on the sediment surface or amongst plants in relatively  
 305 shallow water and grow during the warm season (late spring through to early autumn) (Tokeshi,  
 306 1995). At Hawes Water, calcium carbonate is currently precipitated within the upper 2 metres  
 307 of the water column, from mid-June to mid-August, when the surface waters become super-  
 308 saturated with respect to calcite (Marshall et al., 2008). We can therefore be confident that the  
 309 carbonate and chironomid larval head capsules formed under similar conditions of temperature  
 310 and lake-water isotope composition.

311  
 312 We combine the equation for the temperature-dependence of oxygen-isotope fractionation  
 313 between calcite and water (Kim and O'Neil, 1997) (equation 1) with that between chironomid  
 314 head capsules and water from Lombino et al. (2021) (equation 2) in order to derive a  
 315 fractionation between calcite and chironomid head capsules (equation 3). We then use this  
 316 relationship along with oxygen-isotope values from chironomid head capsules and co-  
 317 occurring calcite in order to reconstruct past water temperature for the Hawes Water sequence.

318  
 319 
$$1000\ln\alpha_{\text{calcite-water}} = 18.03 (\pm 0.36) (10^3 T^{-1}) - 32.42 (\pm 1.22) \quad (1)$$

320 
$$1000\ln\alpha_{\text{chironomid-water}} = 6.29 (\pm 1.86) (10^3 T^{-1}) + 1.16 (\pm 6.46) \quad (2)$$

321 
$$1000\ln\alpha_{\text{calcite-chironomid}} = 1000(\ln\alpha_{\text{calcite-water}} - \ln\alpha_{\text{chironomid-water}}) = 11.74 (\pm 1.89) (10^3 T^{-1}) - 33.58$$
  
 322 
$$(\pm 6.58) \quad (3)$$

323  
 324 The value of  $\alpha_{\text{calcite-chironomid}}$  for each pair of measurements is given by  $(\delta^{18}\text{O}_{\text{carbonate}} +$   
 325  $1000)/(\delta^{18}\text{O}_{\text{chironomid}} + 1000)$ , with both delta values on the VSMOW scale. This value can then  
 326 be entered into Equation (3), suitably rearranged to give a value for T in kelvins, which can  
 327 then be converted to °C. As a test of the accuracy and effectiveness of the method's application  
 328 to fossil material, temperatures inferred from oxygen isotopes in this way can be compared

329 with independent temperature reconstructions derived from the chironomid assemblages from  
330 Hawes Water (Bedford et al. 2004).

331

332 The Late Glacial  $\delta^{18}\text{O}_{\text{chironomid}}$  record from Hawes Water core HW2 extends from the Late  
333 Glacial interstadial through the Younger Dryas stadial and into the earliest Holocene (Fig. 4).

334 The record begins with low  $\delta^{18}\text{O}_{\text{chironomid}}$  values,  $\sim 12.8$  ‰ VSMOW reaching a maximum of

335  $\sim 16.8$  ‰ before declining to  $\sim 14.5$  ‰ immediately before the start of the stadial.  $\delta^{18}\text{O}_{\text{chironomid}}$

336 values fall as low as  $11.5$  ‰ during the Younger Dryas before increasing to  $\sim 14$  ‰ in the Early

337 Holocene. The form of the  $\delta^{18}\text{O}_{\text{chironomid}}$  record agrees closely with the  $\delta^{18}\text{O}_{\text{carbonate}}$  record from

338 HW2. The two records are largely coherent ( $r^2 = 0.70$ ,  $P < 0.05$ ,  $n = 44$ ) and we note also that

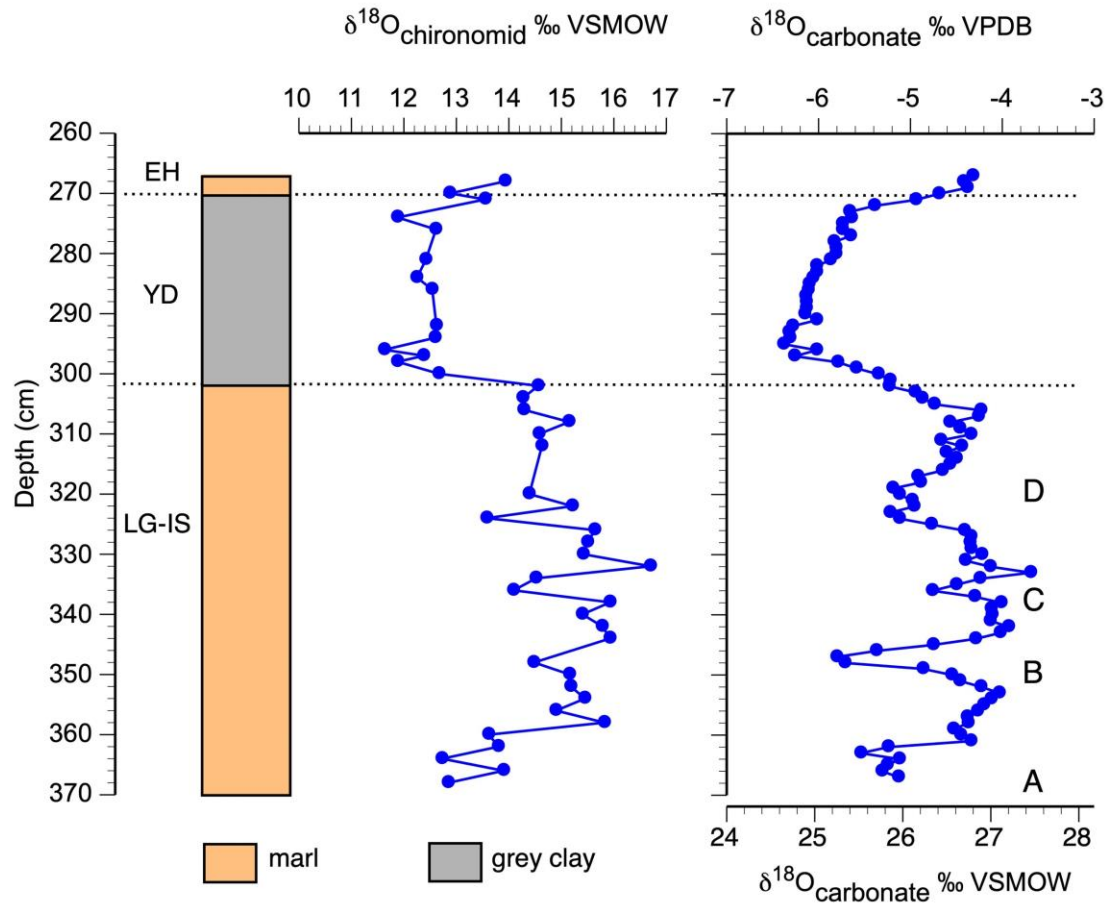
339 the negative excursions in the  $\delta^{18}\text{O}_{\text{carbonate}}$  record (labelled “A” to “D” on Fig. 4) are also evident

340 in the  $\delta^{18}\text{O}_{\text{chironomid}}$  data. Despite broad similarity between the  $\delta^{18}\text{O}_{\text{chironomid}}$  and  $\delta^{18}\text{O}_{\text{carbonate}}$

341 records, we note that the overall amplitude of change over the Late Glacial is much larger for

342 the former ( $\sim 5$  ‰) than the latter ( $\sim 3$  ‰).

343



344

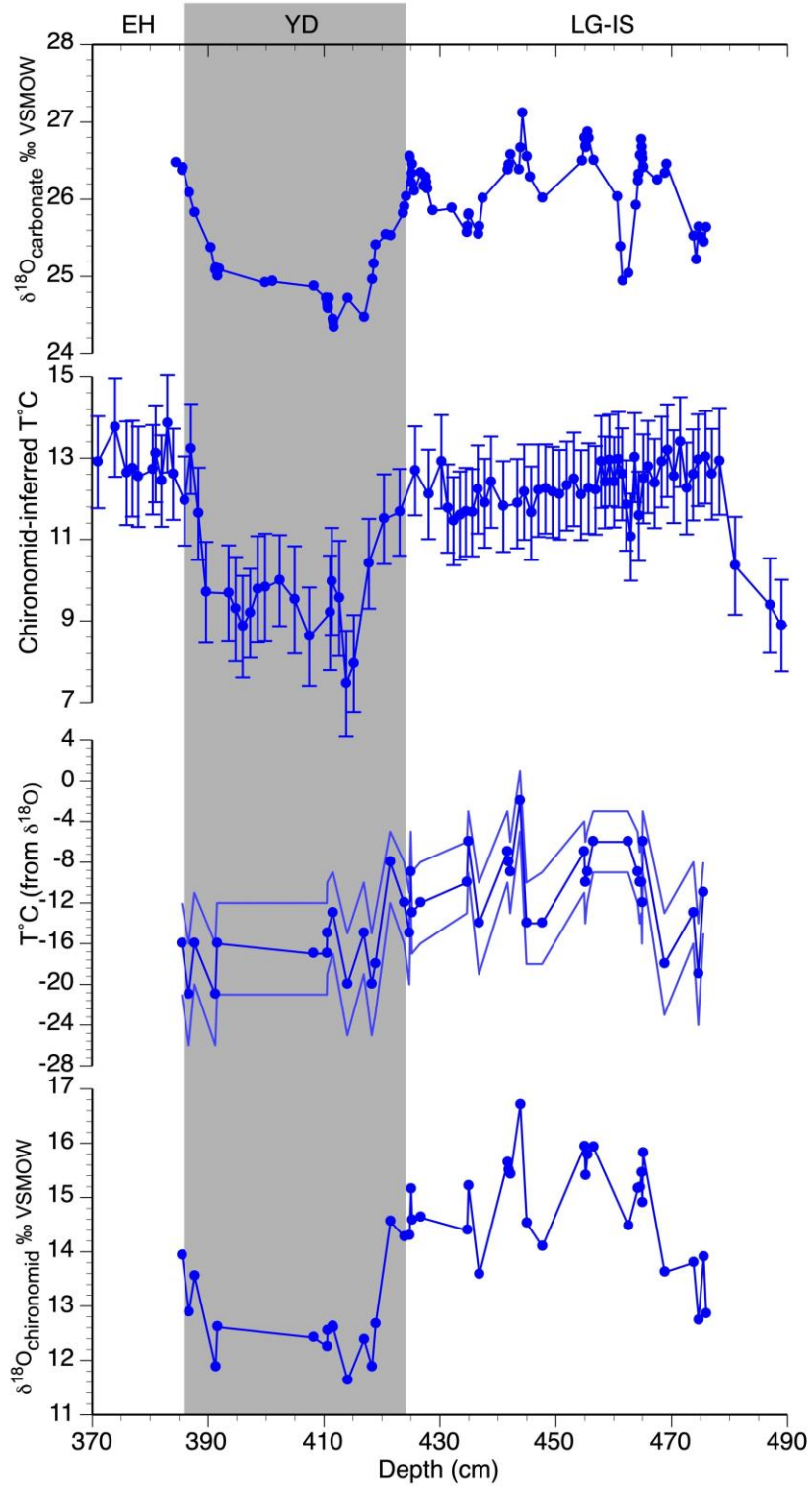
345

346 Fig. 4. Oxygen-isotope stratigraphy ( $\delta^{18}\text{O}_{\text{chironomid}}$  and  $\delta^{18}\text{O}_{\text{carbonate}}$ ) for core HW2 (on the  
 347 original depth scale). Negative excursions in the  $\delta^{18}\text{O}_{\text{carbonate}}$  record are labelled A to D. LG-IS  
 348 = Late Glacial interstadial; YD = Younger Dryas stadial; EH = Early Holocene.

349

350 The palaeotemperatures reconstructed from the  $\delta^{18}\text{O}_{\text{chironomid}}$  and  $\delta^{18}\text{O}_{\text{carbonate}}$  values using the  
 351 method described above are implausibly low, ranging between about  $-20$  and  $-4^\circ\text{C}$  (Fig. 5).  
 352 Comparison of the chironomid-isotope reconstructed temperatures with those inferred by  
 353 transfer function from chironomid assemblages (Fig. 5) shows that the isotope-derived values  
 354 are more variable than the faunal estimates, but still preserve — in a relative way — the main  
 355 features of the stadial-interstadial-stadial climatic sequence. However, the range in values from

356 stadial to interstadial shown by the isotope-derived estimates is 14°C, more than twice the  
357 faunal estimate of 6°C.



358

359

360 Fig. 5.  $\delta^{18}\text{O}_{\text{chironomid}}$ , temperature inferred from the chironomid oxygen isotopes and  $\delta^{18}\text{O}_{\text{carbonate}}$   
361 from core HW2 (plotted on the depth scale of HW1); chironomid-inferred temperatures ( $\pm 1$   
362 SD) from core HW1/2 are from Bedford et al. (2004). Uncertainties ( $\pm 1$  SD) in the isotope-  
363 inferred palaeotemperature values (shown by pale lines) were propagated from the statistical  
364 uncertainties in equations (1) and (2) and analytical errors for  $\delta^{18}\text{O}_{\text{chironomid}}$  and  $\delta^{18}\text{O}_{\text{carbonate}}$   
365 determinations. Note that  $\delta^{18}\text{O}_{\text{carbonate}}$  values are shown relative to the VSMOW scale. LG-IS  
366 = Late Glacial Interstadial; YD = Younger Dryas Stadial; EH = Early Holocene. Transfer of  
367 HW2 data to the HW1 depth scale is explained in the Supplementary Data.

368

369 The Py-GC-MS analyses (Table 1) show that the modern and fossil head capsules responded  
370 differently to pretreatment and, moreover, show contrasting composition. The modern heads  
371 became relatively enriched in chitin upon pretreatment, due to removal of fatty acids, whereas  
372 proteins were removed only to a relatively small extent. By contrast, the three fossil samples  
373 tested were relatively poorer in both proteinaceous material and chitin than the modern  
374 analogue. In addition, the fossil heads contained a relatively high abundance of aliphatic  
375 geopolymers, which were lacking from the modern specimens (Table 1).

376

377

378

379

380

381

382

383 **Table 1.** Relative abundances of bio- and geopolymers in chironomid head capsules based on  
 384 the abundances of their pyrolysis products. Sample numbers for fossil material from Hawes  
 385 Water refer to sample depths in HW/2.

386

	Modern heads		Fossil heads					
			358 cm		360 cm		364 cm	
	untreated	treated	untreated	treated	untreated	treated	untreated	treated
Chitin	0.36	0.53	0.30	0.23	0.34	0.18	0.40	0.28
Fatty acids	0.17	0.01	0.01	0.04	0.02	0.05	0.01	0.05
Proteins	0.47	0.46	0.37	0.17	0.24	0.17	0.36	0.24
Aliphatic geopolymers	0.00	0.00	0.32	0.56	0.40	0.59	0.23	0.43

387

388

#### 389 **4. Discussion**

390 The chironomid-carbonate palaeothermometer is based on four assumptions: 1)  $\delta^{18}\text{O}_{\text{chironomid}}$  is  
 391 a reliable combined proxy for  $\delta^{18}\text{O}_{\text{H}_2\text{O}}$  and temperature, and that the contribution of each to the  
 392  $\delta^{18}\text{O}_{\text{chironomid}}$  record can be reliably quantified; 2) both independent  $\delta^{18}\text{O}$  archives formed  
 393 simultaneously from waters with a common  $\delta^{18}\text{O}_{\text{H}_2\text{O}}$  and water temperature (i.e. in the same  
 394 part of the water column and at the same time of year); 3) sample materials are free from  
 395 contamination; and 4) sample materials are free from post-depositional alteration. The  
 396 unrealistic sub-zero summer temperature estimates from Hawes Water  $\delta^{18}\text{O}_{\text{chironomid}}$  imply that  
 397 at least one of these assumptions is not valid. We now evaluate each of them in turn.

398

399 As discussed in 2.3 above, the relationship between  $\delta^{18}\text{O}_{\text{chironomid}}$  and  $\delta^{18}\text{O}_{\text{H}_2\text{O}}$  is strong and has  
 400 been confirmed through a number of field- and lab-based studies. The impact of temperature  
 401 on  $\alpha_{\text{chironomid-water}}$  in Lombino et al. (2021), however, represents only a single study and requires  
 402 further confirmation. There is some evidence for temperature-dependent oxygen-isotope  
 403 fractionation in cellulose, a biomolecule that shows similar isotopic behaviour to chitin

404 (Beuning et al., 1997, 2002): both cellulose and chitin have previously been regarded as  
405 showing no temperature dependence in oxygen-isotope fractionation (Mayr et al., 2015;  
406 Wooller et al., 2004, 2008; Wolfe et al. 2001, 2007). However, even if we assume a constant  
407  $\alpha_{\text{chironomid-H}_2\text{O}}$  value and then use this in conjunction with  $\delta^{18}\text{O}_{\text{carbonate}}$  values, the reconstructed  
408 temperatures are still unrealistically low and show poor agreement with the chironomid-  
409 inferred temperature estimates. In short, our findings would be unchanged if this approach were  
410 taken.

411

412 The chironomids and carbonate are both very likely to have formed under the same conditions  
413 of water temperature and water-isotope composition (i.e. in the near-surface waters of the lake  
414 during late spring and summer). For the carbonate, this is confirmed by the detailed monitoring  
415 of Hawes Water (Marshall et al., 2007) summarized in 2.1 above. For the chironomids, there  
416 are numerous studies that confirm that the larval chitin forms in late spring to early autumn  
417 (Tokeshi, 1995). Although the larvae live in the surface sediments and plants, they tend to be  
418 confined to shallower water, with conditions of temperature and  $\delta^{18}\text{O}_{\text{H}_2\text{O}}$  similar to those for  
419 carbonate formation.

420

421 Sample contamination is unlikely to be a problem for either  $\delta^{18}\text{O}_{\text{chironomid}}$  or  $\delta^{18}\text{O}_{\text{carbonate}}$ . The  
422 preparation method for carbonate at Hawes Water yields estimates for water temperature that  
423 are realistic for the modern lake when applied to contemporary carbonate (Marshall et al.,  
424 2007). For the chironomids, our evaluation of preparation methods suggests that this will not  
425 have led to any significant effect on the  $\delta^{18}\text{O}_{\text{chironomid}}$  signal and the checks undertaken during  
426 sample preparation confirm the absence of sedimentary contamination (see Supplementary  
427 Material). This leaves only post-depositional alteration of the oxygen isotope ratios of one or  
428 both sample materials as a possible source of error. There is no evidence that post-depositional

429 diagenesis of marl in Hawes Water has led to significant alteration of  $\delta^{18}\text{O}_{\text{carbonate}}$  (Marhsall et  
430 al, 2007), whereas chitin is an organic polymer that might be subject to degradation or other  
431 diagenetic processes.

432

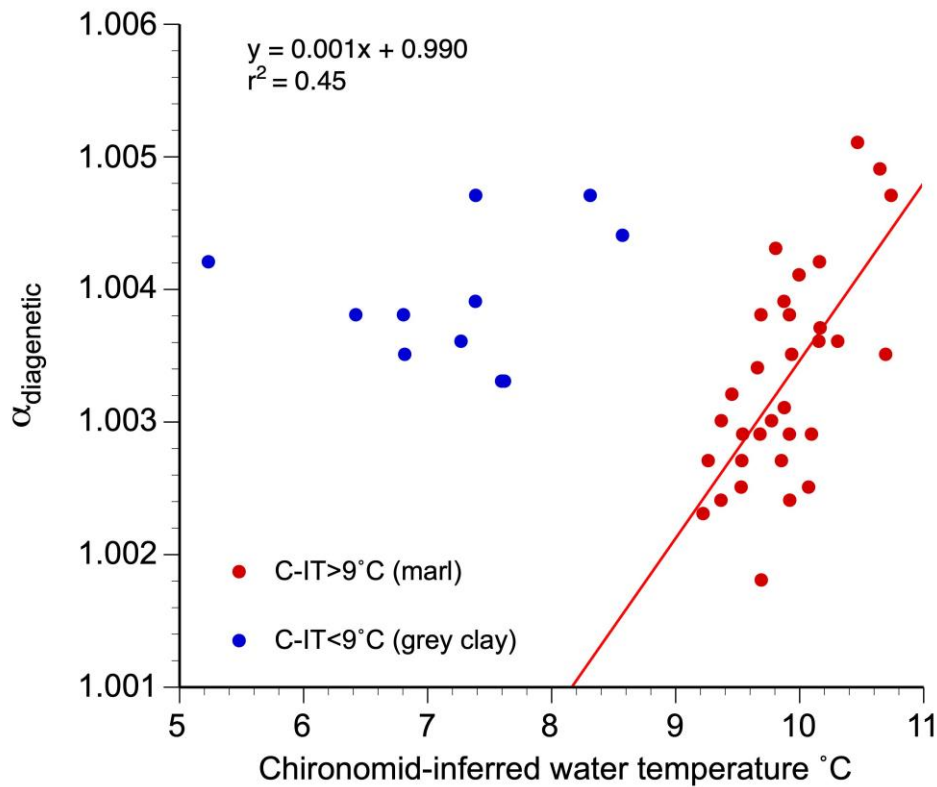
433 The chemical composition of chitin is thought to remain largely unchanged for tens of  
434 thousands of years under favourable depositional environments (e.g. high sedimentation rates  
435 and anoxia) (Stankiewicz et al., 1997a; 1997b). However, the chromatographic screening of  
436 chironomid remains from Hawes Water shows they have lower proportions of both  
437 proteinaceous material and chitin than the modern analogue. Furthermore, the macromolecular  
438 structure of the tested chironomid remains from Hawes Water is characteristic of the formation  
439 of aliphatic (geo)polymers during diagenesis, via the polymerization of liberated lipid  
440 molecules (Baas et al., 1995; Cody et al., 2011; Gupta et al., 2009; Stankiewicz et al., 2000).  
441 Pretreatment had the effect of relatively enriching these geopolymers, whereas proteins and  
442 chitin became depleted (Table 1).

443

444 The conditions governing such geopolymerization are largely unknown and therefore the  
445 influence of the formation of geopolymers on the  $\delta^{18}\text{O}_{\text{chironomid}}$  signature at Hawes Water is  
446 difficult to ascertain, but clearly diagenetic alterations have the potential to reset, or at least  
447 alter, the original  $\delta^{18}\text{O}_{\text{chironomid}}$  signature. We combined the chironomid-inferred and isotope-  
448 derived temperatures presented above to estimate the amount of fractionation that may have  
449 occurred during diagenesis at each level in the core for which paired measurements are  
450 available. We emphasize that these estimates are based on the difference between the  
451 chironomid-inferred and isotope-derived temperatures: we did not attempt to estimate the  
452 degree of diagenetic fractionation based on the Py-GC-MS data, which are, in any case, only  
453 available from three sample levels. Instead, we use the compositional data as evidence that

454 alterations consistent with diagenesis have occurred. The average inferred diagenetic  
455 fractionation using this approach is  $1.0035 \pm 0.0008$  (1 SD); i.e. there is an inferred  $+3.5 \pm 0.8$   
456 ‰ change in  $\delta^{18}\text{O}_{\text{chironomid}}$  values during diagenesis. We plot the calculated diagenetic  
457 fractionation against chironomid-inferred temperature in order to explore any influence of  
458 temperature on the diagenetic process (Fig. 6) and note that the data fall into two apparent  
459 populations. For chironomid-inferred water temperatures  $<9^\circ\text{C}$ , there is no relationship  
460 between temperature and diagenetic fractionation whereas there is a strong positive  
461 relationship for chironomid-inferred water temperatures  $>9^\circ\text{C}$ . In general, the positive  
462 fractionation suggests a loss of  $^{16}\text{O}$  during the geo-polymerization process. The relationship  
463 with ambient temperature is difficult to explain, although we note that those levels for which a  
464 correlation between temperature and diagenetic fractionation exists are from marl sediments  
465 whereas the levels for which the correlation is absent are from clays. The positive diagenetic  
466 fractionation is consistent with early diagenesis, presumably mediated by bacteria within the  
467 marl: we speculate that this diagenetic process may have been delayed in the less permeable  
468 clays, which would account for the lack of correlation with ambient temperature at the time of  
469 deposition or shortly afterwards. The amount of diagenetic fractionation is sensitive to  
470  $\alpha_{\text{chironomid-water}}$ , although different values of  $\alpha_{\text{chironomid-water}}$  would not change the overall patterns  
471 observed, nor our interpretations of them.

472



473

474

475 Fig. 6. Diagenetic fractionation factor ( $\alpha_{\text{diagenetic}}$ ) versus chironomid-inferred water temperature  
 476 (C-IT) for Hawes Water core HW2. Water temperature was determined by subtracting 2.3°C  
 477 from chironomid-inferred air temperature (Marshall et al., 2007). The regression equation and  
 478  $r^2$  value relate only to C-IT values >9°C.

479

480 The partial persistence of proteins after the treatments implies that they contribute to the  
 481  $\delta^{18}\text{O}_{\text{chironomid}}$  values obtained, although their oxygen content is smaller than that of chitin.  
 482 However, there is relatively less protein and chitin than geopolymer in the head capsule  
 483 material following treatment. The diagenetic fractionation must therefore be associated with  
 484 the formation of the geopolymer. Despite this, the coherence between the two independent  $\delta^{18}\text{O}$   
 485 records (i.e. carbonate and chironomid head capsules) suggest that some form of environmental  
 486 signal is still preserved even after diagenesis.

487

## 488 **5. Conclusions**

489 Previous work has shown that the oxygen-isotope composition of chironomid head capsules is  
490 determined primarily by the composition of the environmental water in which the chironomids  
491 lived, but is also dependent on temperature and on the oxygen isotopic composition of the  
492 dominant food source (van Hardenbroek et al., 2018; Lombino et al., 2021). We have shown,  
493 from a Late Glacial lake sediment record from Hawes Water, that a time series of oxygen-  
494 isotope values from chironomid head capsules strongly resembles records based on two other  
495 independent climatic proxies, namely the  $\delta^{18}\text{O}$  of endogenic carbonate and temperatures  
496 inferred from chironomid assemblages using transfer functions. These similarities suggest that  
497  $\delta^{18}\text{O}_{\text{chironomid}}$  records have considerable potential for future studies, especially in lakes that lack  
498 carbonate deposition or preservation, but in which other biomolecules are preserved. However,  
499 in our record the isotopic composition of the head capsules appears to have been altered during  
500 diagenesis, with this additional, unknown fractionation producing unrealistic results in  
501 temperature reconstructions. It is a matter for future research to establish whether such  
502 diagenesis is common in lake sediment settings. A possible relationship between sediment type  
503 and the extent of diagenetic alteration of chironomid head capsules that is evident in our data  
504 requires further investigation. While the apparently orderly diagenetic modification of the  
505 marl-encased head capsules militates for early diagenesis that is closely related to temperature,  
506 the discrepancy with the clay-encased material indicates that the rate of diagenesis is dependent  
507 on the sedimentary context and may be delayed and slowed in low-permeability materials. This  
508 implies that the present results are likely only to be mirrored in a general way in other lakes or  
509 water bodies, and that the diagenetic fractionation factors we have deduced should not be taken  
510 to apply to any sites other than Hawes Water. Nonetheless, our results do indicate that oxygen-  
511 isotope values of chironomid head capsules from Quaternary sequences should be interpreted  
512 with care, especially if the isotope data are to be used in quantitative reconstructions of past

513 climate. Further testing of this ‘combined isotope’ approach could involve oxygen-isotope  
514 analyses of modern carbonate precipitates and head capsules from living chironomid larvae  
515 from a site in which water temperature and water isotope composition are closely monitored.

516

#### 517 **Contributor roles**

518 AL led the investigation and produced the initial draft of the manuscript. AL, DRG, JM, KN  
519 and ZT undertook the analytical work. SB and VJ supervised the work. TA and JH finalized  
520 the manuscript and led the data analysis. All authors contributed to drafting and finalizing the  
521 manuscript. Co-authors are listed alphabetically.

522

#### 523 **Acknowledgements**

524 Funding was provided by a research studentship (NE/H008160/1) from the UK Natural  
525 Environment Research Council to AL. We thank G. Everett Lasher for providing some of the  
526 modern chironomid and water-isotope data used to construct figure 3 and Abigail Hill for help  
527 with R code. We dedicate this paper to the memory of Dr Richard T. Jones, a physical  
528 geographer at the University of Exeter, who died in 2018. Richard’s research included work  
529 on Late Glacial climate records from north-west England and he was responsible for recovering  
530 the core material from Hawes Water that was used in this study. We hope very much that he  
531 would have approved of our efforts.

532

#### 533 **Supplementary Data**

534 Supplementary materials related to this article can be found at <http://...>

535

#### 536 **References**

- 537 Baas, M., Briggs, D.E.G., van Heemst, J.D.H., Kear, A.J. & de Leeuw, J.W., 1995, Selective  
538 preservation of chitin during the decay of shrimp: *Geochimica et Cosmochimica Acta*, 59, 945–  
539 951.
- 540 Bakke, J., Lie, O., Heegaard, E., Dokken, T., Haug, G.H., Birks, H.H., Dulski, P. & Nilsen, T.,  
541 2009. Rapid oceanic and atmospheric changes during the Younger Dryas cold period. *Nature*  
542 *Geoscience*, 2, 202–205.
- 543 Bedford, A. Jones, R., Lang B., Brooks, S. & Marshall, J.D., 2004, A Late-glacial chironomid  
544 record from Hawes Water, northwest England: *Journal of Quaternary Science*, 19, 281–290.
- 545 Beuning, K.R.M., Kelts, K., Ito, E. & Johnson, T.C., 1997, Paleohydrology of Lake Victoria,  
546 East Africa, inferred from  $^{18}\text{O}/^{16}\text{O}$  ratios in sediment cellulose. *Geology* 25, 1083–1086.
- 547 Beuning, K.R.M., Kelts, K., Russell, J. & Wolfe, B.B., 2002. Reassessment of Lake Victoria -  
548 Upper Nile River paleohydrology from oxygen isotope records of lake-sediment cellulose.  
549 *Geology* 30, 559–562.
- 550 Brooks, S.J. & Langdon, P.G., 2014, Summer temperature gradients in northwest Europe  
551 during the Lateglacial to early Holocene transition (15–8 ka BP) inferred from chironomid  
552 assemblages. *Quaternary International*, 341, 80–90.
- 553 Chang, J.C., Shulmeister, J., Gröcke, D.R. & Woodward, C.A., 2018. Toward more accurate  
554 temperature reconstructions based on oxygen isotopes of subfossil chironomid head-capsules  
555 in Australia. *Limnology and Oceanography*, 63, 295–307.
- 556 Cody, G.D., Gupta, N.S., Briggs, D.E.G., Kilcoyne, A.L.D., Summons, R.E., Kenig, F.,  
557 Plotnick, R.E. & Scott, A.C., 2011, Molecular signature of chitin-protein complex in Paleozoic  
558 arthropods: *Geology*, 39, 255–258.
- 559 Gupta, N.S., Cody, G.D., Tetlie, O.E., Briggs, D.E.G., & Summons, R.E., 2009, Rapid  
560 incorporation of lipids into macromolecules during experimental decay of invertebrates:  
561 Initiation of geopolymer formation: *Organic Geochemistry*, 40, 589–594.
- 562 Hammarlund, D., Barnekow, L., Birks, H.J.B., Buchardt, B. & Edwards, T.W.D., 2002,  
563 Holocene changes in atmospheric circulation recorded in the oxygen-isotope stratigraphy of  
564 lacustrine carbonates from northern Sweden. *Holocene*, 12, 339–351.
- 565 Heyng, A., Mayr, C., Lücke, A., Wissel, H. & Striewski, B. 2014, Late Holocene hydrologic  
566 changes in northern New Zealand inferred from stable isotope values of aquatic cellulose in  
567 sediments from Lake Pupuke. *Journal of Paleolimnology*, 51. 458-497.
- 568 Jones, R.T., Marshall, J.D., Crowley, S.F., Bedford, A., Richardson, N., Bloemendal, J. &  
569 Oldfield, F., 2002, A high resolution, multiproxy Late-glacial record of climate change and  
570 intrasystem responses in northwest England. *Journal of Quaternary Science*, 17, 329–340.
- 571 Jones, R., Marshall, J., Fisher, E., Hatton, J., Patrick, C., Anderson, K., Lang, B., Bedford, A.,  
572 Oldfield, F. 2011, Controls on lake level in the early to mid Holocene, Hawes Water,  
573 Lancashire, UK. *Holocene*, 21, 1061–1072.
- 574 Kim, S.T. & O'Neil, J.R., 1997, Equilibrium and nonequilibrium oxygen isotope effects in  
575 synthetic carbonates. *Geochimica et Cosmochimica Acta*, 61, 3461–3475.

- 576 Kim, S. Coplen, T. Horita, J., 2015, Normalization of Stable Isotope Data for Carbonate  
577 Minerals: Implementation of IUPAC Guidelines. *Geochimica et Cosmochimica Acta*, 158,  
578 276–289.
- 579 Lane, C.S., Brauer, A., Blockley, S.P.E. & Dulski, P., 2013, Volcanic ash reveals time-  
580 transgressive abrupt climatic change during the Younger Dryas. *Geology*, 41, 1251–1254.
- 581 Lang, B., Bedford, A., Brooks, S.J., Jones, R.T., Richardson, N., Birks, H.J.B. & Marshall,  
582 J.D., 2010, Early-Holocene temperature variability inferred from chironomid assemblages at  
583 Hawes Water, northwest England. *Holocene*, 20, 943–954.
- 584 Lasher, G.E., Axford, Y., McFarlin, J.M., Kelly, M.A., Osterberg, E.C. & Berkelhammer,  
585 M.B., 2017, Holocene temperatures and isotopes of precipitation in Northwest Greenland  
586 recorded in lacustrine organic materials. *Quaternary Science Reviews*, 170, 45–55.
- 587 Leng, M.J. & Barker, P.A., 2006, A review of the oxygen isotope composition of lacustrine  
588 diatom silica for palaeoclimate reconstruction. *Earth-Science Reviews*, 75, 5–27.
- 589 Leng, M.J. & Marshall, J.D., 2004, Palaeoclimate interpretation of stable isotope data from  
590 lake sediment archives: *Quaternary Science Reviews*, 23, 811–831.
- 591 Lombino, A.G., 2015, The systematics of oxygen isotopes in chironomids: a tool for  
592 reconstructing past climate. Unpublished PhD thesis, University College London, UK.  
593 (available at <https://ethos.bl.uk/OrderDetails.do?did=1&uin=uk.bl.ethos.654622>)
- 594 Lombino, A.G., Atkinson, T.C., Brooks, S.J., Gröcke, D.R., Holmes, J.A., Jones, V.J., 2021,  
595 Experimental determination of the temperature dependence of oxygen-isotope fractionation  
596 between water and chitinous head capsules of chironomid larvae. *Journal of Paleolimnology*,  
597 doi.org/10.1007/s10933-021-00191-z
- 598 Lowe, J.J., Rasmussen, S.O., Björck, S., Hoek, W.Z., Steffensen, J.P., Walker, M.J.C., Yu,  
599 Z.C. & INTIMATE Group members, 2008, Synchronisation of palaeoenvironmental events in  
600 the North Atlantic region during the Last Termination: a revised protocol recommended by the  
601 INTIMATE group. *Quaternary Science Reviews*, 27, 6–17.
- 602 Marshall, J.D., Jones, R.T., Crowley, S.F., Oldfield, F., Nash, S. & Bedford, A., 2002, A high  
603 resolution Late-Glacial isotopic record from Hawes Water, Northwest England Climatic  
604 oscillations: calibration and comparison of palaeotemperature proxies. *Palaeogeography*  
605 *Palaeoclimatology Palaeoecology*, 185, 25–40.
- 606 Marshall, J.D., Lang, B., Crowley, S.F., Weedon, G.P., van Calsteren, P., Fisher, E.H., Holme,  
607 R., Holmes, J.A., Jones, R.T., Bedford, A., Brooks, S.J., Bloemendal, J., Kiriakoulakis, K.,  
608 Ball, J.D. 2007,. Terrestrial impact of abrupt changes in the North Atlantic thermohaline  
609 circulation: Early Holocene, UK. *Geology*, 35, 639-642.
- 610 Mayr, C., Laprida, C., Lücke, A., Martín, R.S., Massaferró, J., Ramón-Mercau, J. & Wissel,  
611 H., 2015, Oxygen isotope ratios of chironomids, aquatic macrophytes and ostracods for lake-  
612 water isotopic reconstructions. Results of a calibration study in Patagonia. *Journal of*  
613 *Hydrology*, 529, 600–607.

- 614 Menzel, D., Van Bergen, P.F., Veld, H., Brinkhuis, H. & Sinninghe Damsté, J.S., 2005, The  
615 molecular composition of kerogen in Pliocene Mediterranean sapropels and associated  
616 homogeneous calcareous ooze. *Organic Geochemistry* 36, 1037–1053.
- 617 North Greenland Ice Core Project members, 2004, High-resolution record of Northern  
618 Hemisphere climate extending into the last interglacial period. *Nature* 431, 147–151.
- 619 Smith, G.G., Sudhakar Reddy, G. & Boon, J.J., 1988, Gas chromatographic-mass  
620 spectrometric analysis of the Curie-point pyrolysis products of some dipeptides and their  
621 diketopiperazine. *Journal of the Chemical Society-Perkin Transactions 2*, 203–211.
- 622 Stankiewicz, B.A. Briggs, D.E.G., Evershed, R.P., Flannery, M.B. & Wuttke, M., 1997a,  
623 Preservation of chitin in 25-million-year-old fossils: *Science*, 276, 1541–1543.
- 624 Stankiewicz, B.A, Briggs, D.E.G., Evershed, R.P. & Duncan, I.J., 1997b, Chemical  
625 preservation of insect cuticle from the Pleistocene asphalt deposits of California, USA:  
626 *Geochimica et Cosmochimica Acta*, 61, 2247–2252.
- 627 Stankiewicz, B.A. Briggs, D.E.G., Michels, R., Collinson, M.E., Flannery, M.B. & Evershed,  
628 R.P., 2000, Alternative origin of aliphatic polymer in kerogen: *Geology*, 28, 559–562.
- 629 Stankiewicz, B.A., Van Bergen, P.F., Duncan, I.J., Carter, J.F., Briggs, D.E.G. & Evershed,  
630 R.P., 1996, Recognition of chitin and proteins in invertebrate cuticles using analytical  
631 pyrolysis/gas chromatography/mass spectrometry. *Rapid Communications in Mass*  
632 *Spectrometry* 10, 1747–1757.
- 633 Stuiver, M. & Reimer P.J., 1993, Extended  $^{14}\text{C}$  data base and revised CALIB 3.0  $^{14}\text{C}$  age  
634 calibration program. *Radiocarbon* 35, 215–30.
- 635 Thomas, Z.A., 2014, Prospects for the detection of tipping points in palaeoclimate records.  
636 Unpublished PhD Thesis, University of Exeter, UK
- 637 Tokeshi, M., 1995, Life cycles and population dynamics. In: Armitage PD, Cranston PSD &  
638 Pinder LCV [eds] *The Chironomidae: biology and ecology of non-biting midges*. Chapman &  
639 Hall, London. pp. 225–268.
- 640 van Hardenbroek, M., Chakraborty, A., Davies, K.L., Harding, P., Heiri, O., Henderson,  
641 A.C.G., Holmes, J.A., Lasher, G.E., Leng, M.J., Panizzo, V.N., Roberts, L., Schilder, J.,  
642 Trueman, C.N. & Wooller, M.J., 2018, The stable isotope composition of organic and inorganic  
643 fossils in lake sediment records: Current understanding, challenges, and future directions.  
644 *Quaternary Science Reviews*, 196, 154–176.
- 645 Verbruggen, F., Heiri, O., Reichart G.J. & Lotter, A.F., 2010, Chironomid  $\delta^{18}\text{O}$  as a proxy for  
646 past lake water  $\delta^{18}\text{O}$ : a Lateglacial record from Rotsee (Switzerland). *Quaternary Science*  
647 *Reviews*, 29, 2271–2279.
- 648 Verbruggen, F., Heiri, O., Reichart G.J., Blaga, C. & Lotter, A.F., 2011, Stable oxygen isotopes  
649 in chironomid and cladoceran remains as indicators for lake water  $\delta^{18}\text{O}$ . *Limnology and*  
650 *Oceanography*, 56, 2071–2079.

- 651 Wang, Y.V., O'Brien, D.M., Jenson, J., Francis, D. & Wooller, M.J., 2009, The influence of  
652 diet and water on the stable oxygen and hydrogen isotope composition of Chironomidae  
653 (Diptera) with paleoecological implications. *Oecologia*, 160, 225–233.
- 654 Wiik, E., Bennion, H., Sayer, C.D., Davidson, T.A., McGowan, S., Patmore, I.R. & Clarke,  
655 S.J., 2015, Ecological sensitivity of marl lakes to nutrient enrichment: evidence from Hawes  
656 Water, UK. *Freshwater Biology*, 60, 2226–2247.
- 657 Wolfe, B.B., Edwards, T.W. & Elgood, R., 2001, Carbon and oxygen isotope analysis of lake  
658 sediment cellulose: methods and applications. In: *Tracking environmental change using lake*  
659 *sediments* (Vol. 1), Last, W.M. & Smol, J.P. (Eds), Kluwer Academic Publishers, Dordrecht:  
660 373–400.
- 661 Wolfe, B.B., Falcone, M.D., Clogg-Wright, K.P., Mongeon, C.L., Yi, Y., Brock, E., Amour,  
662 N.A.S., Mark, W.A. & Edwards, T.W.D., 2007, Progress in isotope paleohydrology using lake  
663 sediment cellulose. *Journal of Paleolimnology*, 37, 221–231.
- 664 Wooller, M., Wang, Y. & Axford, Y., 2008, A multiple stable isotope record of Late  
665 Quaternary limnological changes and chironomid paleoecology from northeastern Iceland.  
666 *Journal of Paleolimnology*, 40, 63–77.
- 667 Wooller, M.J., Francis, D., Fogel, M.L., Miller, G.H., Walker, I.R. & Wolfe, A.P., 2004,  
668 Quantitative paleotemperature estimates from  $\delta^{18}\text{O}$  of chironomid head capsules preserved in  
669 arctic lake sediments. *Journal of Paleolimnology*, 31, 267–274.
- 670  
671

**Declaration of interests**

The authors declare that they have no known competing financial interests or personal relationships that could have appeared to influence the work reported in this paper.

The authors declare the following financial interests/personal relationships which may be considered as potential competing interests:

**Climate reconstruction from paired oxygen-isotope analyses of chironomid larval head capsules and endogenic carbonate (Hawes Water, UK) - potential and problems**

Alex Lombino, Tim Atkinson, Stephen J. Brooks, Darren R. Gröcke, Jonathan Holmes, Vivienne J. Jones, Jim D. Marshall, Klaas G.J. Nierop, Zoë Thomas

**Contributor roles**

AL led the investigation and produced the initial draft of the manuscript. AL, DRG, JM, KN and ZT undertook the analytical work. SB and VJ supervised the work. TA and JH finalized the manuscript and led the data analysis. All authors contributed to drafting and finalizing the manuscript. Co-authors are listed alphabetically.



Click here to access/download

**e-Component/Supplementary data**  
**Supplementary\_file\_1\_REVISED.docx**

